Neurobiology of Aging 35 (2014) 1002–1011

Contents lists available at ScienceDirect

Neurobiology of Aging

journal homepage: www.elsevier.com/locate/neuaging

Age-related downregulation of the $CaV_{3.1}$ T-type calcium channel as a mediator of amyloid beta production

Rachel A. Rice, Nicole C. Berchtold, Carl W. Cotman, Kim N. Green*

Department of Neurobiology and Behavior, Institute for Memory Impairments and Neurological Disorders, University of California, Irvine, CA, USA

ARTICLE INFO

Article history:
Received 28 May 2013
Received in revised form 7 October 2013
Accepted 25 October 2013
Available online 30 October 2013

Keywords:
Aging
Alzheimer's disease
Calcium
T-type calcium channel
APP processing
Amyloid
Calpains

ABSTRACT

Alzheimer's is a crippling neurodegenerative disease that largely affects aged individuals. Decades of research have highlighted age-related changes in calcium homeostasis that occur before and throughout the duration of the disease, and the contributions of such dysregulation to Alzheimer's disease pathogenesis. We report an age-related decrease in expression of the $CaV_{3.1}$ T-type calcium channel at the level of messenger RNA and protein in both humans and mice that is exacerbated with the presence of Alzheimer's disease. Downregulating T-type calcium channels in N2a cells and the 3xTg-AD mouse model of Alzheimer's disease, by way of pharmacologic inhibition with *NNC-55-0396*, results in a rapid increase in amyloid beta production via reductions in non-amyloidogenic processing, whereas genetic overexpression of the channel in human embryonic kidney cells expressing amyloid precursor protein produces complementary effects. The age-related decline in $CaV_{3.1}$ expression may therefore contribute to a pro-amyloidogenic environment in the aging brain and represents a novel opportunity to intervene in the course of Alzheimer's disease pathogenesis.

1. Introduction

As Alzheimer's disease (AD) disproportionately affects the aged population, it is imperative to understand what changes in the brain with aging to allow for the accumulation of pathology and subsequent deficits in cognition. Cellular calcium dyshomeostasis is an established hallmark of both aging and Alzheimer's disease, and is thought to play a role in not only disease initiation, but also progression (Green, 2009; Landfield and Pitler, 1984; Lopez et al., 2008). Age- and disease-related changes in various calcium channels, receptors, and pumps have been shown to contribute to changes in processing of the amyloid precursor protein (APP), namely increases in production of the toxic amyloid beta peptide (Aβ) (Green et al., 2008; Oules et al., 2012). Such an increase in Aβ levels can further increase calcium dyshomeostasis in a vicious, feed-forward cycle, ultimately resulting in cell death (Demuro et al., 2011; Resende et al., 2008) While discrete components of calcium signaling have been studied, a comprehensive overview of age- and AD-related changes in components of calcium signaling has not been carried out to date. We have queried a human microarray data set that demonstrates the breadth of changes in calcium-related genes between young nondemented (20–59) and aged nondemented (74–95) individuals, and aged non-demented (74–95) and demented (74–95) individuals. Moreover, we have identified a dramatic and consistent age-related reduction in the expression of the *cacna1g* gene, which encodes the $CaV_{3.1}$ T-type calcium channel. A further reduction in expression of *cacna1g* is observed with AD, identifying this gene as a potential mediator of calcium dysregulation that contributes to cognitive decline.

Heretofore, T-type calcium channels have been largely unexplored in the context of Alzheimer's disease. While the expression and activity of high-voltage activated calcium (HVAC) channels such as L-type channels are known to change with age, and these channels have been historically implicated in AD-associated calcium dysregulation, T-type calcium channels represent a unique class of voltage-activated calcium channels (Anekonda et al., 2011; Thibault and Landfield, 1996). T-type calcium channels are expressed widely throughout the brain, and in other excitable cells of the body and constitute a group of low voltage-activated calcium channels composed of 3 different subtypes—$CaV_{3.1}$, $CaV_{3.2}$, and $CaV_{3.3}$, encoded by the genes *cacna1g*, *cacna1h*, and *cacna1i*, respectively. Unlike HVAC channels, T-type calcium channels require only minimal membrane depolarizations and conduct modest amounts of Ca^{2+} into the cell. As a result of their gating kinetics, a subset of T-type channels remain tonically active at resting membrane potential, allowing Ca^{2+} to flow into the cell. Because T-type calcium channels conduct small amounts of calcium

* Corresponding author at: Department of Neurobiology and Behavior, Institute for Memory Impairments and Neurological Disorders, 3208 Biological Sciences III, University of California, Irvine, Irvine, CA 92697-4545. Tel.: +1 949 824 3859.
E-mail address: kngreen@uci.edu (K.N. Green).

0197-4580/$ – see front matter © 2014 Elsevier Inc. All rights reserved.
http://dx.doi.org/10.1016/j.neurobiolaging.2013.10.090

into the cell near resting membrane potential and further depolarize the membrane, HVAC channels may become activated as a result (Perez-Reyes, 2003). Because of these properties, T-type calcium channels have been described as being "ideally suited for regulating neuronal excitability" (Iftinca, 2011). Currently, T-type calcium channel blockers are found to be ameliorative for a variety of conditions including epilepsy, essential tremor, and neuropathic pain, and the roles these channels play in autism, vasodilation, sleep cycle regulation, and tumor cell cycle regulation continue to be investigated (Anderson et al., 2005; Astori et al., 2011; Brodie et al., 2012; Dogrul et al., 2003; Oshima et al., 2005; Quesada et al., 2011; Rim et al., 2012; Splawski et al., 2006).

The significance of understanding the consequences of age- and AD-related T-type channel downregulation is three-fold. First, as researchers are investing efforts into blocking T-type channels toward the goal of managing the previously mentioned conditions, it is critical to know if the $CaV_{3.1}$ channel is a target that disappears with age, rendering T-type calcium channel blockers less effective. Second, Food and Drug Administration (FDA)-approved T-type channel blockers such as trimethadione and ethosuximide already exist for absence seizures and more indications in which T-type calcium channels are implicated are becoming apparent, calling for further investigation in humans. It is critical to understand if administration of T-type blockers to humans is creating a pro-amyloidogenic environment in the brain, as this could render an individual more susceptible to developing AD. Finally, if $CaV_{3.1}$ downregulation is a major initiating factor for the increased production of the toxic Aβ peptide, then the $CaV_{3.1}$ T-type calcium channel represents a novel target for preventative therapeutics in Alzheimer's disease.

2. Methods

2.1. Human microarray data

2.1.1. Human tissue samples

Human tissue samples were obtained and RNA purified as previously described (Berchtold et al., 2008). Briefly, tissue samples were taken from 58 individuals categorized as nondemented young (20–59), nondemented aged (74–95), or Alzheimer's disease (74–95). Brain regions included entorhinal cortex (EC), hippocampus (HC), posterior cingulate gyrus (PCG), and superior frontal gyrus (SFG).

2.1.2. Microarray analysis

Microarray analysis and validation was carried out as previously described (Berchtold et al., 2008). A correlation test was performed with GraphPad Prism software Version 5 to determine the degree of correlation between age and *cacna1g* messenger RNA (mRNA) expression level.

2.2. Immunoblot assays

2.2.1. Western blot of brain homogenates

Half brains were flash frozen on dry ice following extraction from mice. The cerebellum was removed and the remaining brain was homogenized in 150 mg/mL tissue protein extraction reagent (Thermo Scientific Rockford, IL, USA) with complete mini protease inhibitor cocktail tablets (Roche Indianapolis, IN, USA) and phosphatase 2 inhibitor cocktail (Sigma-Aldrich St.Louis, MO, USA). Homogenates were subsequently centrifuged at 44,000 rpm for 1 hour at 4 °C, yielding soluble protein fractions. A protein quantification assay was performed to determine protein concentration of each sample (Bio-Rad Hercules, CA, USA). Twenty micrograms of protein were loaded per well with reducing agent and sample buffer. For quantification of $CaV_{3.1}$ expression in nontransgenic and triple transgenic (3xTg-AD) mice, protein homogenates were run on 3%–8% Tris-Acetate gels with Tris-Acetate SDS running buffer (Invitrogen). All other samples were run on 4%–12% Bis-Tris gels with MES SDS running buffer (Invitrogen). Proteins were transferred to 0.02 μm nitrocellulose membranes, which were blocked in 5% nonfat milk in tris-buffered saline supplemented with 0.2% tween-20. Membranes were probed with specific primary antibodies. Primary antibodies used were: rabbit anti-$CaV_{3.1}$ (1:1000, Alomone, Jerusalem, Israel), rabbit anti-CT20 APP for full length APP, C99, C89, and C83 (1:3000, Calbiochem), rabbit anti-ADAM10 (1:1000, Millipore), rabbit anti-BACE (1:1000, Millipore), mouse anti-HT7 (1:1000, Pierce), mouse anti-AT270 (1:1000, Pierce), rabbit anti-phospho Tau ser199/202 (1:1000, Millipore), rabbit anti-Cdk5 (Millipore), mouse anti-GSK-3β (BD Biosciences), rabbit anti-phospho GSK-3α/β ser21/9 (Cell Signaling), rabbit anti-p35 C-terminus, mouse anti-spectrin (Millipore), rabbit anti-calpain 1 (1:1000, Cell Signaling), rabbit anti-calpain 2 (1:1000, Cell Signaling), rabbit anti-actin (1:10,000, Sigma-Aldrich), rabbit anti-GAPDH (1:10,0000, Sigma-Aldrich). Membranes were incubated with goat anti-rabbit (1:10,000, Sigma-Aldrich) or goat anti-mouse (1:5000, Sigma-Aldrich) HRP-conjugated secondary antibodies for visualization. Steady state levels of protein expression were quantified via densitometric analysis and normalized to actin or GAPDH expression.

2.2.2. Western blot of cell lysates

N2a and HEK269 cells were rinsed with ice-cold phosphate buffered saline and lysed in mammalian protein extraction reagent (Thermo Scientific) with complete mini protease inhibitor tablet (Roche) by centrifuging at 14,000 rpm for 10 minutes at 4 °C. Protein concentration of samples was determined as stated in the previous section. Twenty micrograms of protein were loaded into each well of 4%–12% Bis-Tris Gels and gels were run with MES SDS running buffer (Life Technologies, Grand Island, NY, USA). Gels were transferred and probed as described previously. Primary antibodies used were: rabbit anti-$CaV_{3.1}$ (previously mentioned), rabbit anti-CT20 for C99, C89, and C83 (previously mentioned), rabbit anti-ADAM 10 (previously mentioned), mouse anti-secreted APPα (1:500, Wako Richmond, VA, USA), and rabbit anti-actin (previously mentioned).

2.3. Immunohistochemistry analysis

2.3.1. DAB analysis

Half of each mouse brain was drop-fixed in 4% paraformaldehyde and subsequently cryopreserved in 30% sucrose. Frozen half brains were sectioned at 40 μm on a freezing microtome. Free-floating sections were incubated in 30% H_2O_2 with methanol to quench endogenous peroxidase and then treated with 70% formic acid for 4 minutes. Sections were blocked in tris-buffered saline supplemented with 0.1% Triton X100 (Sigma-Aldrich) and 2% bovine serum albumen (Sigma-Aldrich). Sections were incubated in mouse anti-6E10 (1:1000, Sigma-Aldrich) overnight and incubated with anti-mouse HRP-conjugated secondary (1:10,000, Sigma-Aldrich) supplemented with normal horse serum (Vector Labs Burlingame, CA, USA). Deposition of 3,3′-Diaminobenzidine (DAB) precipitate was achieved using the VECTASTAIN Elite ABC system (Vector Labs).

2.3.2. Thioflavin-S analysis

Cryopreserved tissue sections were mounted on slides and allowed to dry overnight. Mounted tissue was washed in descending ethanol concentrations (100%, 95%, 70%, 50%) and incubated in 0.5% Thioflavin S (Sigma-Aldrich) solution in 50% ethanol. Slides

were coverslipped and imaged on a Leica confocal microscope using Z-stacks. These stacks were then analyzed using Bitplane Imaris 7.42, to calculate the number and volumes of plaques.

2.3.3. Immunofluorescence analysis

Half of each mouse brain was drop-fixed in 4% paraformaldehyde and subsequently cryopreserved in 30% sucrose. Frozen half brains were sectioned at 40 μm on a freezing microtome. Free-floating sections were blocked in PBS supplemented with 0.2% Triton X100 (Sigma-Aldrich) and 5% goat serum (Sigma-Aldrich) and then incubated overnight at 4 °C in human anti-HT7 (1:1000, Thermo Scientific) in blocking solution. Sections were incubated in Alexafluor 555 secondary antibody in the dark and subsequently mounted on slides and coverslipped. Images were taken in comparable areas of the hippocampus of each animal using a Leica confocal microscope and analyzed using ImageJ software Version 10.2.

2.4. Enzyme-linked immunosorbent assay (ELISA) analysis

2.4.1. ELISA analysis of brain homogenates

Soluble protein fractions were generated from half brains as described in section 2.2.1. The remaining pellet was solubilized in half the volume of the initial pellet in TPER in 70% formic acid and centrifuged again at 44,000 rpm for 1 hour at 4 °C to yield an insoluble protein fraction. $A\beta_{1\text{-}40}$ and $A\beta_{1\text{-}42}$ levels were measured in the soluble and insoluble fractions as described in Green et al., 2008.

2.4.2. ELISA analysis of media from cell culture

Growth medium from N2a cells treated with NNC-55-0396 (Tocris Bioscience, Bristol, UK) for 8 or 24 hours was collected at the time of cell collection and soluble $A\beta_{1\text{-}40}$ and $A\beta_{1\text{-}42}$ levels were measured as described in Green et al., 2008.

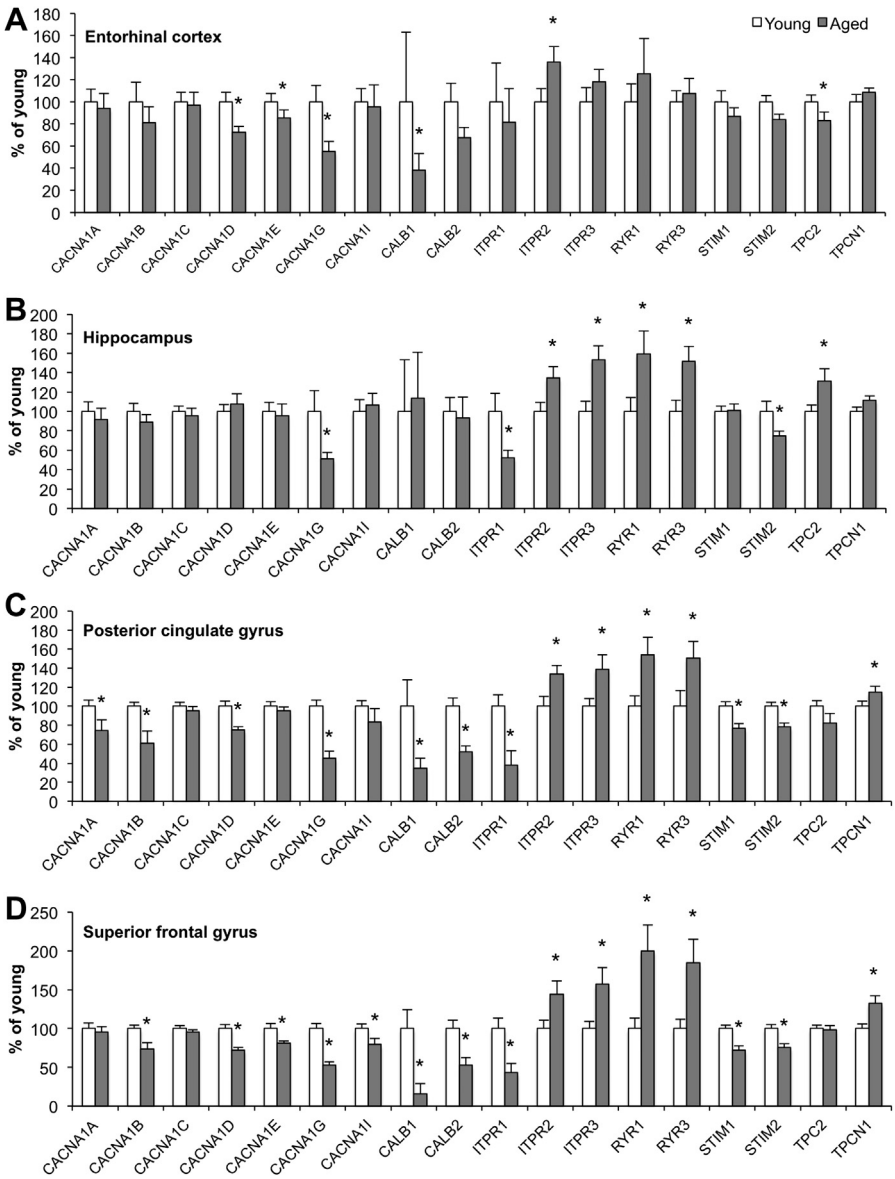

Fig. 1. Human microarray data analysis of calcium-related genes as a function of age. Human microarray database included samples from young nondemented (20–59) and aged nondemented (74–95) individuals. Gene expression values for a single probe set for each gene are normalized to young controls in 4 different areas of the brain: entorhinal cortex (A; n = 21 young, 9 aged), hippocampus (B; n = 18 young, 16 aged), posterior cingulate gyrus (C; n = 18 young, 15 aged), and superior frontal gyrus (D; n = 22 young, 16 aged). See supplementary file for data for all gene probe sets. Errors bars represent standard error of the mean. * $p < 0.05$.

Table 1
Expression levels of human *cacna1g* as a function of age. Expanded data with all 3 probes reveal significant decreases in *cacna1g* expression in all 4 brain areas

Probe	211315_s_at	210380_s_at	207869_s_at
EC			
Young	100.00	100.00	100.00
Aged	52.38[a]	42.54[b]	47.88[a]
HC			
Young	100.00	100.00	100.00
Aged	75.46[a]	54.02[a]	48.54 ($p = 0.058$)
PCG			
Young	100.00	100.00	100.00
Aged	62.10[c]	55.81[c]	54.45[c]
SFG			
Young	100.00	100.00	100.00
Aged	62.86[c]	55.23[c]	50.31[c]

Key: EC, entorhinal cortex; HC, hippocampus; PCG, posterior cingulated gyrus; SFG, superior frontal gyrus.
[a] $p < 0.05$.
[b] $p < 0.01$.
[c] $p < 0.001$.

2.5. Cell cultures

N2a (Neuro 2A, ATCC) and HEK269 (APP expressing) cells were maintained in Dulbecco's Modified Eagle Medium (Invitrogen) supplemented with 10% fetal bovine serum (Invitrogen) and 1% penicillin/streptomycin (Invitrogen). Cells were subcultured every 3 days at 70%–80% confluency and were discarded after 20 passages. For treatment, N2a cells were plated in 6-well plates at 300,000 cells/well (8 hour treatment) or 200,000 cells/well (24 hour treatment) and treated 24 hours later with PBS or NNC-55-0396 (5 mM stock solution dissolved in 1X PBS) to a final concentration of 8 μM (Tocris Bioscience). Media were collected from the wells at the conclusion of treatment for ELISA analysis.

2.6. Cell transfection

HEK269 cells were transiently transfected with pcDNA or cacna1g cDNA (Origene, Rockville, MD, USA) using Lipofectamine 2000 reagent (Invitrogen). Expression was allowed to proceed for 72 hours before cells were collected.

2.7. Statistics

Analysis of microarray data was performed as previously described (Berchtold et al., 2008). Pearson r and p values for gene expression correlations were calculated using GraphPad Prism software. Student's unpaired t tests were used to determine p values in different treatments groups for the 3xTg-AD mice, N2a cells, and HEK269 cells.

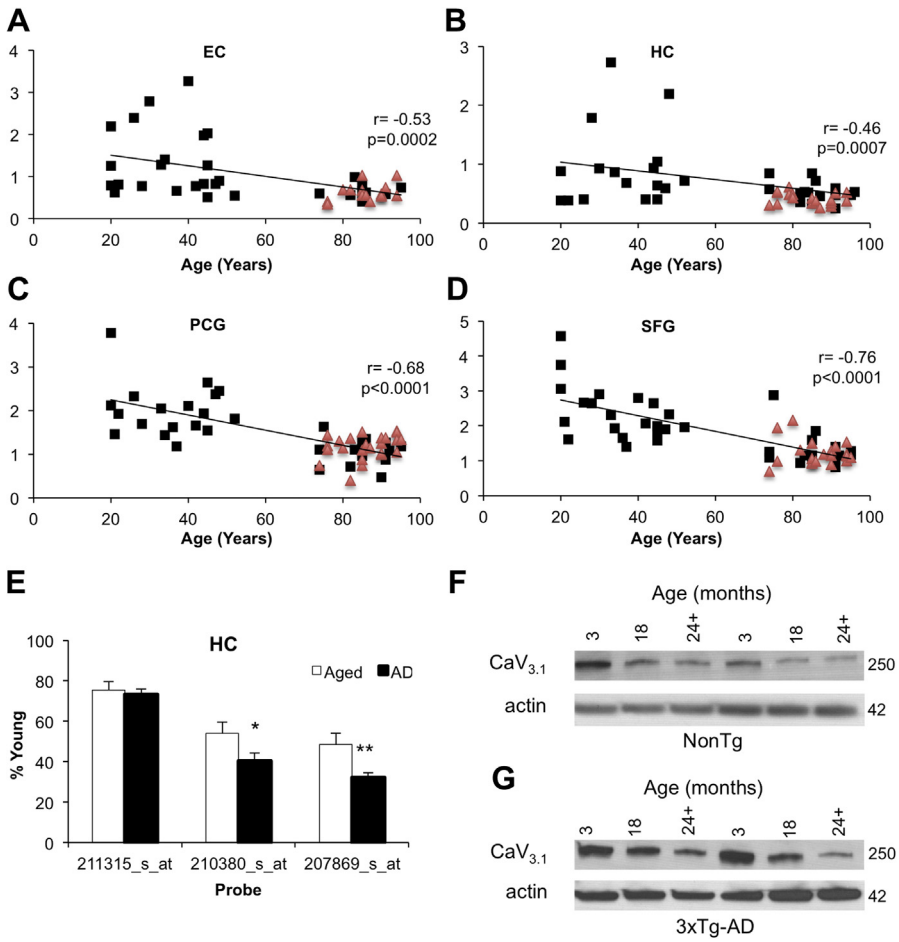

Fig. 2. Correlation between *cacna1g* expression and age and Alzheimer's disease (AD). Significant and inverse relationships exist between age and *cacna1g* expression in the entorhinal cortex (n = 45, $p = 0.0002$), hippocampus (n = 52, $p = 0.0007$), posterior cingulate gyrus (n = 57, $p < 0.0001$), and then superior frontal gyrus (n = 59, $p < 0.0001$) (A–D). Two of 3 probe sets in the hippocampus reveal significant age-related decreases in AD brains compared with aged brains (E; n = 18 AD, n = 16 aged). Steady state levels of the $CaV_{3.1}$ T-type calcium channel are decreased with age in nontransgenic (top) and 3xTg-AD mice (bottom) (F). * $p < 0.05$, ** $p < 0.01$. Abbreviation: AD, Alzheimer's disease.

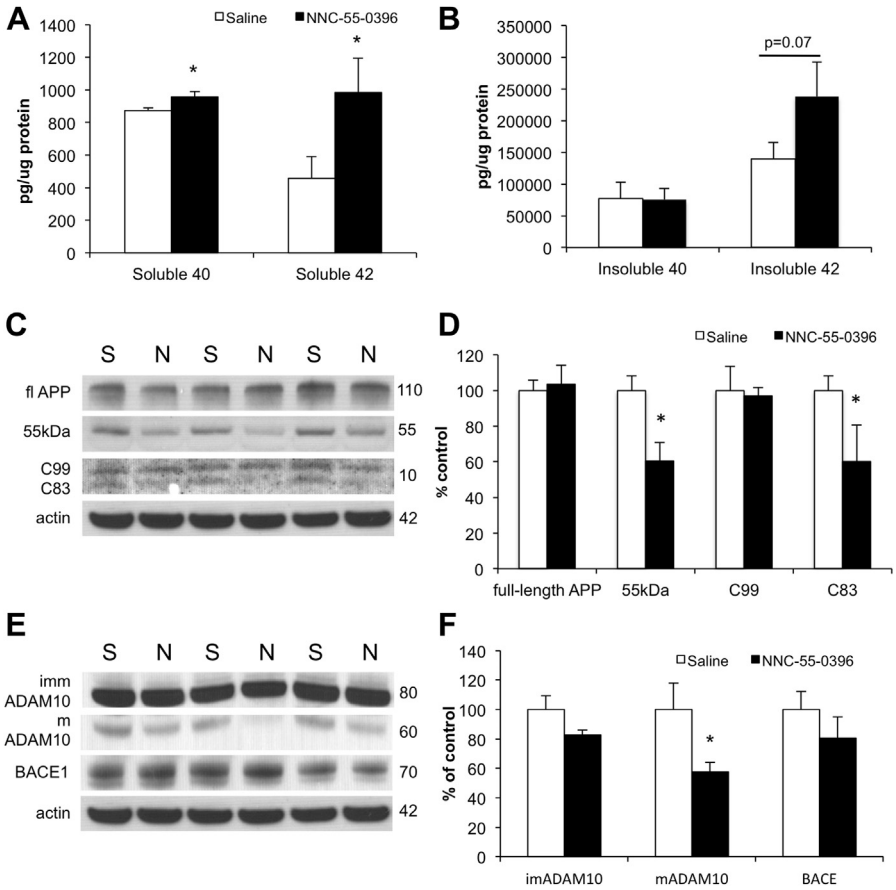

Fig. 3. NNC-55-0396 decreases amyloidogenic processing, resulting in increased Aβ production. Treatment with NNC-55-0396 increased soluble levels of $A\beta_{1\text{-}40}$ and $A\beta_{1\text{-}42}$ in 3xTg-AD mice, while levels of insoluble $A\beta_{1\text{-}42}$ trended toward an increase (A–B). Western blot showed levels of full length amyloid precursor protein (APP) were unchanged with treatment, but a 55kDa C-terminal fragment and C83 were both significantly decreased (C, quantified in D). T-type channel inhibition decreased levels of mature ADAM10, though no changes in immature ADAM10 or BACE1 were found (E, quantified in F). * $p < 0.05$. Abbreviation: APP, amyloid precursor protein.

3. Results

3.1. *Cacna1g* mRNA expression is consistently decreased in the human brain with age

Human microarray data was analyzed for 18 different calcium related genes, in 4 different regions of the brain—the EC, HC, PCG, and SFG. Analyses of a single probe set revealed significant changes in mRNA expression levels with age across the 4 brain regions. Six out of 18 genes were significantly changed with age compared with young controls in the EC, while expression levels of 8 out of 18 genes change with age in the HC (Fig. 1A and B). In the PCG and SFG, most of the genes showed differences in expression levels with age, with 14 of 18 in the former and 15 of 18 in the latter (Fig. 1C and D). Noticeably, the expression levels of most genes decreased with age, though levels of expression for genes encoding ionositol triphosphate receptors (IP_3R) and ryanodine receptors were consistently upregulated across the brain regions surveyed. Aside from expression levels of *calb1*, which encodes calbindin D28k, a calcium binding protein whose expression is known to decrease dramatically with age and Alzheimer's, the expression of *cacna1g*, a gene encoding the $CaV_{3.1}$ T-type calcium channel, was most conspicuously decreased in all 4 brain areas (Riascos et al., 2011; Sequier et al., 1990). mRNA expression levels of this channel were reduced by 41%, 49%, 45%, and 46% in the EC, HC, PCG, and SFG, respectively, when three separate probe sets were collapsed across regions (data no shown). Moreover, expanded data for all 3 RNA probe sets for *cacna1g* revealed consistent reductions in expression (Table 1). As age-related changes in this channel in the brain have not previously been reported or suggested, we sought to determine if such dramatic changes were further exaggerated in the presence of Alzheimer's disease. Analysis revealed significant and inverse correlations between age and *cacna1g* expression. Importantly, this age-related downregulation held true when tissue from individuals with AD were also included (Fig. 2A–D). Moreover, 2 of 3 probes revealed *cacna1g* expression to be significantly decreased in the AD brain compared with aged, nondemented controls in the HC, a region critical for learning and memory that degenerates relatively early in the course of Alzheimer's disease (Fig. 2E) (de Leon et al., 1989).

3.2. Steady state levels of $CaV_{3.1}$ decrease with age in the brains of wild type and 3xTg-AD mice

We wanted to determine if the downregulation of T-type channel mRNA expression held true at the protein level, and going forward, we aimed to manipulate this channel in mice. We therefore assessed steady state levels of $CaV_{3.1}$ by western blot analysis in the 3xTg-AD transgenic mouse model of AD and nontransgenic (NonTg) controls for these mice. We found a robust, age-related decrease in expression of this channel in both nontransgenic controls and 3xTg-AD mice (Fig. 3),

confirming the age-related decline of this channel is maintained at both the mRNA and protein level.

3.3. $CaV_{3.1}$ blockade results in increased Aβ production

To explore the consequences of T-type channel reductions with age, we next used pharmacologic inhibitors of the channels to mimic the aged brain. Female 3xTg-AD mice aged 14–16 month-old were injected intraperitoneally every other day for 2 weeks with 20 mg/kg NNC-55-0396 dissolved in PBS and controls were injected with an equal volume of PBS (saline n = 9; NNC-55-0396 n = 8). NNC-55-0396 is a highly selective T-type calcium channel blocker (7 μM vs. >100μM IC_{50} for $CaV_{3.1}$ T-type vs. L-type calcium channels, respectively). Importantly, NNC-55-0396 is not readily processed by cells to create an active metabolite capable of inhibiting L-type calcium channels, unlike its analog Mibefradil (Huang et al., 2004). The dose was chosen based on previous literature demonstrating efficacy of NNC-55-0396 in a mouse model of essential tremor (Quesada et al., 2011). Despite a relatively short treatment, ELISA analysis revealed significant increases in both $Aβ_{1-40}$ and $Aβ_{1-42}$ in the TPER-soluble fraction of the brain homogenates, and a trend toward an increase ($p = 0.07$) in $Aβ_{1-42}$ in the 70% formic acid-soluble (insoluble) fraction of the brain homogenates (Fig. 4A and B). This increase in Aβ production was accompanied by decreases in the C83 C-terminal fragment of APP, a product of nonamyloidogenic processing, and a 55 kDa C-terminal fragment of APP (Fig. 4C and D). Furthermore, the mature proteolytically active form of the α-secretase ADAM10 was decreased with T-type channel blockade, while no changes in steady state levels of the β–secretase BACE1 were observed with treatment (Fig. 4E and F). It is likely the decrease in mature ADAM10 that underlies the decrease in C83 production. Together, these data demonstrate the T-type channel blockade reduces nonamyloidogenic processing, shifting the equilibrium toward the amyloidogenic processing pathway, and in turn, produces higher levels of the Aβ peptide.

3.4. T-type channel blockade does not alter plaque load in 3xTg-AD mice

We looked by immunohistochemistry to determine if plaque load was altered in mice treated with NNC-55-0396. Probing with 6E10, we did not detect any differences in plaque number in the subiculum, CA1, or entorhinal cortex. We further investigated the number of dense core plaques between saline and NNC-55-0396 treated mice by staining with Thioflavin-S and using BitPlane Imaris software version 7.5.2 to segregate and color code plaques by volume (Fig. 4C is a representative image of a brain slice stained for thio-S and subsequently processed with Imaris). Fig. 4D reveals no significant differences in plaque number between groups, regardless of plaque volume categorization.

3.5. The effects of T-type channel blockade on APP processing are recapitulated in a murine neuroblastoma cell line

To confirm the changes in APP processing in vitro, we treated the murine N2a cell line with 8 μM NNC-55-0396 for 8 and 24 hours. With 8 hours of treatment, soluble $Aβ_{1-42}$ was significantly increased, as determined by a sandwich ELISA (Fig. 5A). By 24 hours, levels of both soluble $Aβ_{1-40}$ and $Aβ_{1-42}$ were significantly increased in cells treated with the T-type channel inhibitor compared with those treated with saline (Fig. 5B). While steady state levels of full-length APP were increased, levels of the C83 C-terminal fragment of APP were dramatically reduced with just 8 hours of treatment with NNC-55-0396 (Fig. 5C). We speculate that the increase in full-length APP is because of reduced cleavage by α-secretase, thereby leaving a larger pool of APP unprocessed. Given that T-type channel inhibition increased Aβ levels and decreased C83 in both the 3xTg-AD mice and the N2a cell line, we sought to determine if the underlying changes in APP processing were maintained in vitro. Indeed, we observed a decrease in mature ADAM10 in cells treated with the blocker, confirming the inhibitory nature of T-

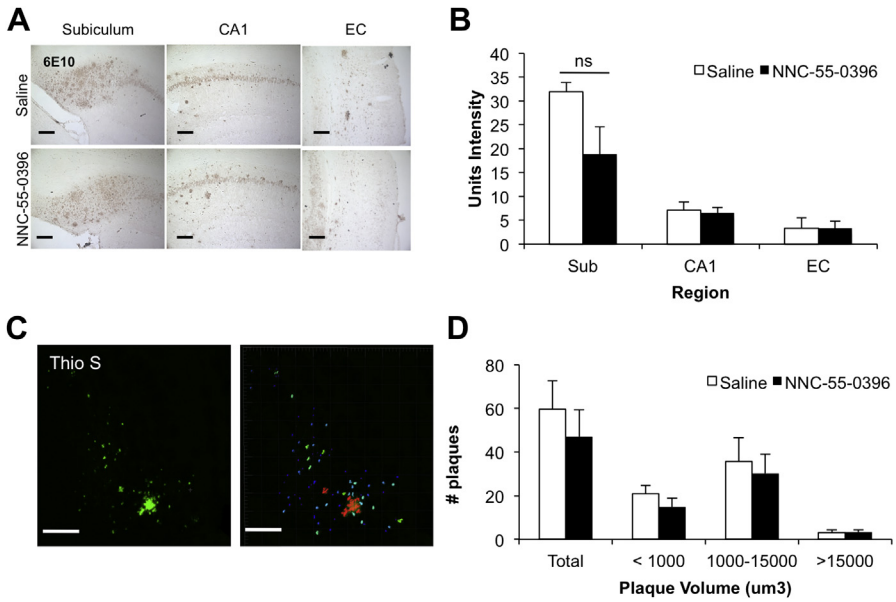

Fig. 4. T-type channel inhibition does not affect plaque load in 3xTg-AD mice. Plaque load as assessed by 6E10 staining in the subiculum (Sub), CA1, and entorhinal cortex (EC) revealed no significant differences between untreated and treated animals (A–B). A representative picture of thioflavin-S staining for dense core plaques on the left, categorized by plaque volume using Imaris BitPlane software on right revealed no significant changes between groups (C–D). Abbreviations: EC, entorhinal cortex; Sub, subiculum.

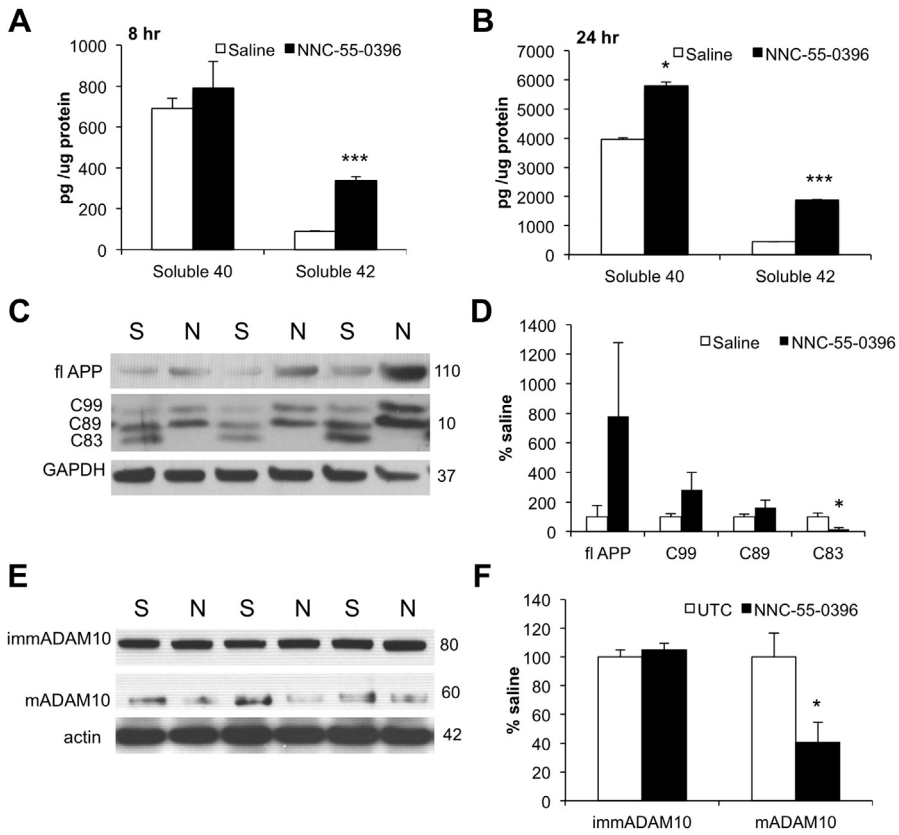

Fig. 5. The effects of NNC-55-0396 are recapitulated in the murine N2a cell line. N2a cells treated with 8 μM NNC-55-0396 for 8 hours secrete significantly more $A\beta_{1\text{-}42}$, while 24 hour treatment results in significant increases in both $A\beta_{1\text{-}40}$ and $A\beta_{1\text{-}42}$ (A–B). Eight hours of T-type channel inhibition insignificantly increases full-length amyloid precursor protein (APP) levels and significantly decreases levels of C83 (C–D). As in the 3xTg-AD mice, decreases in C83 were accompanied by decreases in mature ADAM10, without changes in BACE1 levels with 8 hours of treatment (E–F). * $p < 0.05$, *** $p < 0.001$. Abbreviation: APP, amyloid precursor protein.

type channel blockade on ADAM10 maturation both in vitro and in vivo.

3.6. Overexpression of $CaV_{3.1}$ increases nonamyloidogenic processing in HEK269 cells

We next wanted to ensure that the effects of NNC-55-0396 on APP processing are due to effects on the T-type calcium channels and not an off-target effect of the compound. To determine this, we overexpressed pcDNA or *cacna1g* cDNA in HEK cells expressing APP for 72 hours. We achieved a 74% increase in $CaV_{3.1}$ expression, which coincided with an almost 3-fold increase in secreted APP-α, as measured from media collected at 72 hours (Fig. 6A). As secreted APP-α is a product of α-secretase processing, this suggests that overexpression of the T-type calcium channel increases non-amyloidogenic processing, opposite the effects seen with inhibition. Moreover, a trend toward an increase in mature ADAM10 was also seen with $CaV_{3.1}$ overexpression (Fig. 6A and B). While this change is not statistically significant, it is not entirely surprising, as NNC-55-0396 blocks all 3 T-type calcium channels—$CaV_{3.1}$, $CaV_{3.2}$, and $CaV_{3.3}$—and therefore indicates that $CaV_{3.1}$ is likely not the sole T-type channel mediating the effects on APP processing. We attempted both small interfering RNA and small hairpin RNA knockdown of *cacna1g* in N2a and HEK269 cells, but were unable to achieve robust reductions in steady state levels of the channel, perhaps because of a long half-life or numerous alternative splice variants (Emerick et al., 2006).

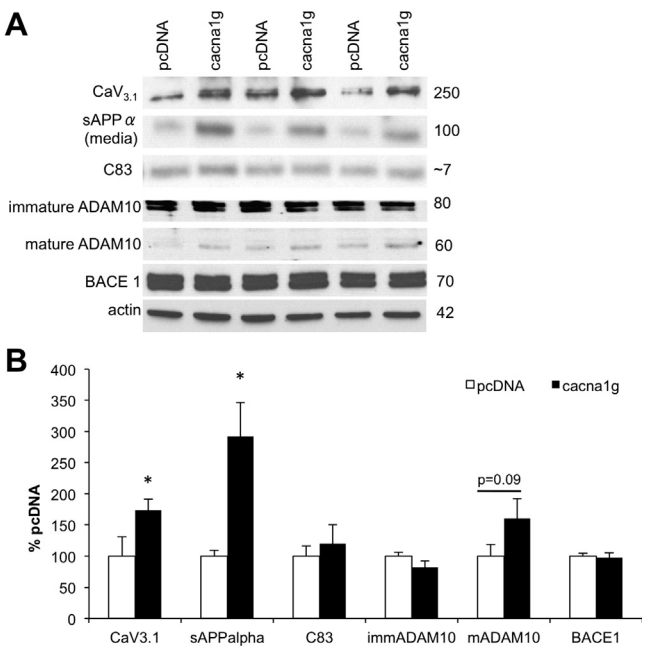

Fig. 6. Overexpression of *cacna1g* produces complementary effects to NNC-55-0396 in HEK69 cells. We achieved a 74% overexpression of the $CaV_{3.1}$ T-type channel in HEK269 cells, which coincided with a significant increase in secreted APPα and a trend toward an increase in mature ADAM10 levels, while BACE1 levels remained unchanged (A, quantified in [B]). * $p \leq 0.05$.

3.7. Short-term T-type channel inhibition does not alter tau phosphorylation, despite decreasing p25

Despite dramatic changes in APP processing seen in 3xTg-AD mice with NNC-55-0396 treatment, there were no observable changes to total or phosphorylated levels of tau. Indeed, no differences were noted when probing with HT7 for total tau, either by western blot or immunofluorescence (Fig. 7A, B, D and E). Likewise, no changes were found when probing with AT270, an antibody recognizing tau phosphorylated at threonine 181, a marker of paired helical filaments. Finally, tau can be phosphorylated at serine 199 by GSK3β and serine 202 by GSK3β, and Cdk5, 2 putative tau kinases (Morioka et al., 2006). An antibody detecting these phosphorylation sites again demonstrated no differences. Finally, levels of GSK3 phosphorylated at serines 9 and 21, an Akt-mediated event that can inhibit GSK3 activity, were unchanged (Fig. 7A) (Cross et al., 1995).

Although we did not find changes in total or phosphorylated levels of tau, nor in total or phosphorylated levels of Cdk5 or GSK3β, we found a striking downregulation in p25 production (Fig. 7C). Typically, p35, a short-lived protein, associates with Cdk5 to limit its activity and location in the cell (Patrick et al., 1998). However, with age and neurodegeneration, increased calpain activity leads to increased cleavage of p35 to p25, a degradation-resistant and promiscuous regulator of Cdk5 that allows for its extended activity and aberrant cellular localization as a kinase, ultimately resulting in tau hyperphosphorylation and neuronal death (Cruz et al., 2003; Patrick et al., 1999). To confirm that this decrease in p25 production was a result of a reduction in calpain activity, we probed for α-spectrin, a 250-kDa protein in the brain that yields a 150-kDa calpain-specific cleavage fragment (Veeranna et al., 2004). We found an 80% reduction in the spectrin breakdown product (SBDP150), indicating a downregulation of calpain-mediated cleavage. Moreover, in probing for steady state levels of calpains, we found a trend toward a reduction in calpain 1 ($p = 0.08$) and a significant reduction in calpain 2, distinguished by the calcium concentrations required for their activity (micromolar and millimolar, respectively). This finding is in line with previous literature reporting that treatment with the T-type channel blocker Mibefradil attenuates calpain 2 transcription at all time points surveyed (1, 3, 7, and 14 days) in the heart after a myocardial infarction, and reduces calpain 1 transcription at 2 of 4 time points (Sandmann et al., 2002).

4. Discussion

We report age-related changes in expression levels in most of the 18 calcium-related genes surveyed across 4 brain regions. In

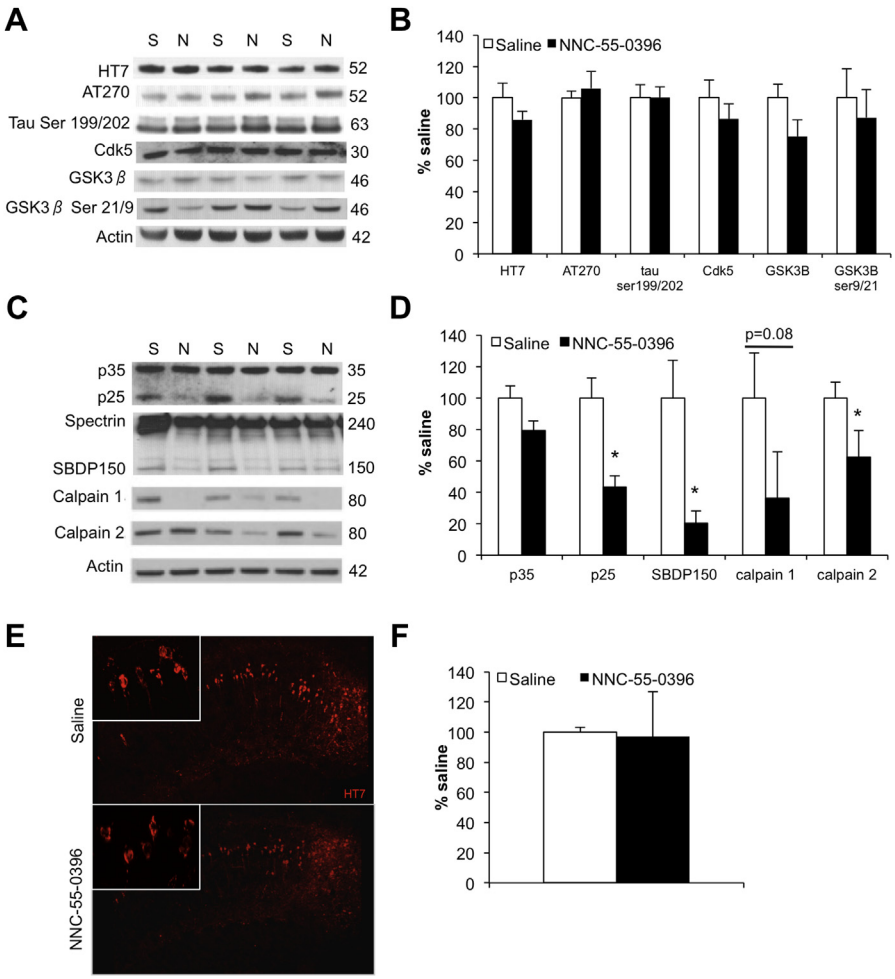

Fig. 7. T-type channel inhibition reduces calpain-mediated cleavage, does not change tau pathology in 3xTg-AD mice. T-type channel inhibition had no effect on total or phosphorylated levels of tau, or total or phosphorylated levels of Cdk5 or GSK3β, as determined by western blotting (A, quantified in [B]). Immunofluorescent staining for HT7 in the hippocampus also revealed no differences (E, quantified in [F]). Levels of p25 and the calpain-specific spectrin breakdown product (SBDP150) were significantly decreased with NNC-55-0396 treatment, likely because of a trend toward a decrease in calpain 1 levels and a significant decrease in calpain 2 levels (C, quantified in [D]).

terms of calcium-related proteins that have already been extensively studied, such as IP_3 and ryanodine receptors and calbindin d28K, our findings from human microarray data are relatively congruent with previously published findings. Expression profiles for genes encoding both IP_3Rs and ryanodine receptors revealed consistent age-related increases, which is in agreement with literature suggesting that augmentations in calcium signaling through both types of endoplasmic reticulum-bound calcium receptors contribute greatly to the calcium dyshomeostasis seen with age and Alzheimer's disease (Chakroborty et al., 2009; Oules et al., 2012; Stutzmann et al., 2006). It is of note that age-related decreases in IP_3R density have been found in the cerebral cortex, albeit in rats (Martini et al., 1994). Of all gene expression levels surveyed, the gene encoding calbindin D28k was most significantly changed. Levels were decreased by between 65% and 79% in the EC, PCG, and SFG. Additionally, both probes for calbindin revealed significant decreases (85% and 86%) in hippocampal tissue from AD brains compared with tissue from aged controls brains (data not shown). These findings are in accordance with the idea that calbindin immunoreactivity is reduced in the hippocampus with AD and correlates with pathology, and cognitive impairment (Iritani et al., 2001; Maguire-Zeiss et al., 1995; Palop et al., 2003). On the whole, our results underscore the extent of age-related changes in calcium handling and lend credence to the calcium hypothesis of Alzheimer's disease.

Focusing more narrowly, our findings inform us that the age-related decreases in $CaV_{3.1}$ expression in the brain, and the use of pharmacologic agents that block this channel, could mediate increases in amyloid production that initiate a cascade of toxic cellular events in the brain. Despite the potentially positive outcomes of T-type blockade for tau pathogenesis, it is widely accepted that Aβ production precedes tau hyperphosphorylation, leading us to postulate that the use of T-type channel inhibitors in the middle-aged adult could produce a highly amyloidogenic environment in the brain that initiates pathogenesis and could not be offset by a concurrent reduction in tau phosphorylation, as this appears to be a downstream event.

Beyond these data serving as a cautionary tale for the use of T-type channel blockers, our findings related specifically to *cacna1g* represent the discovery of another gene capable of mediating age- and AD-related Aβ production, and is a novel opportunity to intervene in the course of aberrant aging processes. Going forward, we aim to identify ways by which expression of the *cacna1g* gene is downregulated with age in the brain, and how we may be able to upregulate expression or activity. Literature from the cancer field identifies *cacna1g* as a tumor suppressor gene and implicates age-related *cacna1g* promoter hypermethylation and the resulting decrease in expression in a variety of peripheral cancers (Garcia-Baquero et al., 2013; Toyota et al., 1999). Interestingly, a novel compound ST101 was found to inhibit Aβ generation and improve cognition in 3xTg-AD mice, and its mechanism of action was recently revealed to be through enhancement of T-type calcium channels (Green et al., 2011; Moriguchi et al., 2012).

Troublingly, support has recently emerged for clinical trials using T-type channel blockers to treat Alzheimer's, after some successes with L-type blockers in animal models of AD, despite disappointing results in human clinical trials (Lopez-Arrieta and Birks, 2000). Moreover, the belief that antihypertensive use reduces the risk dementia remains controversial, and a recent database study of antihypertensives found that while angiotensin converting enzyme inhibitor and beta-blocker use was inversely associated with incident dementia, calcium channel blocker use was positively associated with cognitive deficits (Wagner et al., 2012).

In summary, the efficacy of calcium channel blockers for the prevention or treatment of Alzheimer's disease is not convincing, and more importantly, they may actually lead to deleterious results, including an increased risk of cancer and dementia. Our results suggest that age- and disease-related downregulation of the $CaV_{3.1}$ T-type calcium channel is conducive to amyloid production and that the use of T-type channel blockers should be critically reviewed for its potential as a pro-amyloidogenic agent, at least in patients of middle or older age. Further efforts to understand both what causes the downregulation of and how to enhance the activity of T-type channels in the aged brain may yield novel therapeutic strategies for the prevention of Alzheimer's disease.

Acknowledgements

This work was supported by grants from the Alzheimer's Association and the American Federation for Aging Research to KNG and by NIH AG00538 to CWC.

Appendix A. Supplementary data

Supplementary data associated with this article can be found, in the online version, at http://dx.doi.org/10.1016/j.neurobiolaging.2013.10.090.

References

Anders, A., Gilbert, S., Garten, W., Postina, R., Fahrenholz, F., 2001. Regulation of the alpha-secretase ADAM10 by its prodomain and proprotein convertases. FASEB journal: official publication of the Federation of American Societies for Experimental Biology 15, 1837–1839.

Anderson, M.P., Mochizuki, T., Xie, J., Fischler, W., Manger, J.P., Talley, E.M., Scammell, T.E., Tonegawa, S., 2005. Thalamic Cav3.1 T-type Ca2+ channel plays a crucial role in stabilizing sleep. Proceedings of the National Academy of Sciences of the United States of America 102, 1743–1748. http://dx.doi.org/10.1073/pnas.0409644102.

Anekonda, T.S., Quinn, J.F., Harris, C., Frahler, K., Wadsworth, T.L., Woltjer, R.L., 2011. L-type voltage-gated calcium channel blockade with isradipine as a therapeutic strategy for Alzheimer's disease. Neurobiol Dis 41, 62–70. http://dx.doi.org/10.1016/j.nbd.2010.08.020.

Astori, S., Wimmer, R.D., Prosser, H.M., Corti, C., Corsi, M., Liaudet, N., Volterra, A., Franken, P., Adelman, J.P., Luthi, A., 2011. The Ca(V)3.3 calcium channel is the major sleep spindle pacemaker in thalamus. Proceedings of the National Academy of Sciences of the United States of America 108, 13823–13828. http://dx.doi.org/10.1073/pnas.1105115108.

Berchtold, N.C., Cribbs, D.H., Coleman, P.D., Rogers, J., Head, E., Kim, R., Beach, T., Miller, C., Troncoso, J., Trojanowski, J.Q., Zielke, H.R., Cotman, C.W., 2008. Gene expression changes in the course of normal brain aging are sexually dimorphic. Proceedings of the National Academy of Sciences of the United States of America 105, 15605–15610. http://dx.doi.org/10.1073/pnas.0806883105.

Brodie, M.J., Ben-Menachem, E., Chouette, I., Giorgi, L., 2012. Zonisamide: its pharmacology, efficacy and safety in clinical trials. Acta neurologica Scandinavica Supplementum 194, 19–28. http://dx.doi.org/10.1111/ane.12016.

Chakroborty, S., Goussakov, I., Miller, M.B., Stutzmann, G.E., 2009. Deviant ryanodine receptor-mediated calcium release resets synaptic homeostasis in presymptomatic 3xTg-AD mice. The Journal of neuroscience: the official journal of the Society for Neuroscience 29, 9458–9470. http://dx.doi.org/10.1523/JNEUROSCI.2047-09.2009.

Cribbs, D.H., Berchtold, N.C., Perreau, V., Coleman, P.D., Rogers, J., Tenner, A.J., Cotman, C.W., 2012. Extensive innate immune gene activation accompanies brain aging, increasing vulnerability to cognitive decline and neurodegeneration: a microarray study. Journal of neuroinflammation 9, 179. http://dx.doi.org/10.1186/1742-2094-9-179.

Cross, D.A., Alessi, D.R., Cohen, P., Andjelkovich, M., Hemmings, B.A., 1995. Inhibition of glycogen synthase kinase-3 by insulin mediated by protein kinase B. Nature 378, 785–789. http://dx.doi.org/10.1038/378785a0.

Cruz, J.C., Tseng, H.C., Goldman, J.A., Shih, H., Tsai, L.H., 2003. Aberrant Cdk5 activation by p25 triggers pathological events leading to neurodegeneration and neurofibrillary tangles. Neuron 40, 471–483.

de Leon, M.J., George, A.E., Stylopoulos, L.A., Smith, G., Miller, D.C., 1989. Early marker for Alzheimer's disease: the atrophic hippocampus. Lancet 2, 672–673.

Demuro, A., Smith, M., Parker, I., 2011. Single-channel Ca(2+) imaging implicates Abeta1-42 amyloid pores in Alzheimer's disease pathology. The Journal of cell biology 195, 515–524. http://dx.doi.org/10.1083/jcb.201104133.

Dogrul, A., Gardell, L.R., Ossipov, M.H., Tulunay, F.C., Lai, J., Porreca, F., 2003. Reversal of experimental neuropathic pain by T-type calcium channel blockers. Pain 105, 159–168.

Emerick, M.C., Stein, R., Kunze, R., McNulty, M.M., Regan, M.R., Hanck, D.A., Agnew, W.S., 2006. Profiling the array of Ca(v)3.1 variants from the human

T-type calcium channel gene CACNA1G: alternative structures, developmental expression, and biophysical variations. Proteins 64, 320–342. http://dx.doi.org/10.1002/prot.20877.

Garcia-Baquero, R., Puerta, P., Beltran, M., Alvarez, M., Sacristan, R., Alvarez-Ossorio, J.L., Sanchez-Carbayo, M., 2013. Methylation of a Novel Panel of Tumor Suppressor Genes in Urine Moves Forward Non-Invasive Diagnosis and Prognosis in Bladder Cancer: A Two Center Prospective Study. The Journal of urology. http://dx.doi.org/10.1016/j.juro.2013.01.105.

Green, K.N., 2009. Calcium in the initiation, progression and as an effector of Alzheimer's disease pathology. J Cell Mol Med 13, 2787–2799. http://dx.doi.org/10.1111/j.1582-4934.2009.00861.x.

Green, K.N., Demuro, A., Akbari, Y., Hitt, B.D., Smith, I.F., Parker, I., LaFerla, F.M., 2008. SERCA pump activity is physiologically regulated by presenilin and regulates amyloid beta production. The Journal of cell biology 181, 1107–1116. http://dx.doi.org/10.1083/jcb.200706171.

Huang, L., Keyser, B.M., Tagmose, T.M., Hansen, J.B., Taylor, J.T., Zhuang, H., Zhang, M., Ragsdale, D.S., Li, M., 2004. NNC 55-0396 [(1S,2S)-2-(2-(N-[(3-benzimidazol-2-yl)propyl]-N-methylamino)ethyl)-6-fluo ro-1,2,3,4-tetrahydro-1-isopropyl-2-naphtyl cyclopropanecarboxylate dihydrochloride]: a new selective inhibitor of T-type calcium channels. J Pharmacol Exp Ther 309, 193–199. http://dx.doi.org/10.1124/jpet.103.060814.

Iftinca, M.C., 2011. Neuronal T-type calcium channels: what's new? Iftinca: T-type channel regulation. J Med Life 4, 126–138.

Iritani, S., Niizato, K., Emson, P.C., 2001. Relationship of calbindin D28K-immunoreactive cells and neuropathological changes in the hippocampal formation of Alzheimer's disease. Neuropathology: official journal of the Japanese Society of Neuropathology 21, 162–167.

Kuhn, P.H., Wang, H., Dislich, B., Colombo, A., Zeitschel, U., Ellwart, J.W., Kremmer, E., Rossner, S., Lichtenthaler, S.F., 2010. ADAM10 is the physiologically relevant, constitutive alpha-secretase of the amyloid precursor protein in primary neurons. EMBO J 29, 3020–3032. http://dx.doi.org/10.1038/emboj.2010.167.

Landfield, P.W., Pitler, T.A., 1984. Prolonged Ca2+-dependent afterhyperpolarizations in hippocampal neurons of aged rats. Science 226, 1089–1092.

Lopez, J.R., Lyckman, A., Oddo, S., Laferla, F.M., Querfurth, H.W., Shtifman, A., 2008. Increased intraneuronal resting [Ca2+] in adult Alzheimer's disease mice. Journal of neurochemistry 105, 262–271. http://dx.doi.org/10.1111/j.1471-4159.2007.05135.x.

Maguire-Zeiss, K.A., Li, Z.W., Shimoda, L.M., Hamill, R.W., 1995. Calbindin D28k mRNA in hippocampus, superior temporal gyrus and cerebellum: comparison between control and Alzheimer disease subjects. Brain research Molecular brain research 30, 362–366.

Molloy, S.S., Bresnahan, P.A., Leppla, S.H., Klimpel, K.R., Thomas, G., 1992. Human furin is a calcium-dependent serine endoprotease that recognizes the sequence Arg-X-X-Arg and efficiently cleaves anthrax toxin protective antigen. The Journal of biological chemistry 267, 16396–16402.

Morioka, M., Kawano, T., Yano, S., Kai, Y., Tsuiki, H., Yoshinaga, Y., Matsumoto, J., Maeda, T., Hamada, J., Yamamoto, H., Fukunaga, K., Kuratsu, J., 2006. Hyperphosphorylation at serine 199/202 of tau factor in the gerbil hippocampus after transient forebrain ischemia. Biochemical and biophysical research communications 347, 273–278. http://dx.doi.org/10.1016/j.bbrc.2006.06.096.

Oshima, T., Ozono, R., Yano, Y., Higashi, Y., Teragawa, H., Miho, N., Ishida, T., Ishida, M., Yoshizumi, M., Kambe, M., 2005. Beneficial effect of T-type calcium channel blockers on endothelial function in patients with essential hypertension. Hypertension research: official journal of the Japanese Society of Hypertension 28, 889–894. http://dx.doi.org/10.1291/hypres.28.889.

Oules, B., Del Prete, D., Greco, B., Zhang, X., Lauritzen, I., Sevalle, J., Moreno, S., Paterlini-Brechot, P., Trebak, M., Checler, F., Benfenati, F., Chami, M., 2012. Ryanodine receptor blockade reduces amyloid-beta load and memory impairments in Tg2576 mouse model of Alzheimer disease. The Journal of neuroscience: the official journal of the Society for Neuroscience 32, 11820–11834. http://dx.doi.org/10.1523/JNEUROSCI.0875-12.2012.

Palop, J.J., Jones, B., Kekonius, L., Chin, J., Yu, G.Q., Raber, J., Masliah, E., Mucke, L., 2003. Neuronal depletion of calcium-dependent proteins in the dentate gyrus is tightly linked to Alzheimer's disease-related cognitive deficits. Proceedings of the National Academy of Sciences of the United States of America 100, 9572–9577. http://dx.doi.org/10.1073/pnas.1133381100.

Patrick, G.N., Zhou, P., Kwon, Y.T., Howley, P.M., Tsai, L.H., 1998. p35, the neuronal-specific activator of cyclin-dependent kinase 5 (Cdk5) is degraded by the ubiquitin-proteasome pathway. The Journal of biological chemistry 273, 24057–24064.

Patrick, G.N., Zukerberg, L., Nikolic, M., de la Monte, S., Dikkes, P., Tsai, L.H., 1999. Conversion of p35 to p25 deregulates Cdk5 activity and promotes neurodegeneration. Nature 402, 615–622. http://dx.doi.org/10.1038/45159.

Perez-Reyes, E., 2003. Molecular physiology of low-voltage-activated t-type calcium channels. Physiol Rev 83, 117–161. http://dx.doi.org/10.1152/physrev.00018.2002.

Quesada, A., Bui, P.H., Homanics, G.E., Hankinson, O., Handforth, A., 2011. Comparison of mibefradil and derivative NNC 55-0396 effects on behavior, cytochrome P450 activity, and tremor in mouse models of essential tremor. European journal of pharmacology. http://dx.doi.org/10.1016/j.ejphar.2011.01.004.

Resende, R., Ferreiro, E., Pereira, C., Resende de Oliveira, C., 2008. Neurotoxic effect of oligomeric and fibrillar species of amyloid-beta peptide 1-42: involvement of endoplasmic reticulum calcium release in oligomer-induced cell death. Neuroscience 155, 725–737. http://dx.doi.org/10.1016/j.neuroscience.2008.06.036.

Riascos, D., de Leon, D., Baker-Nigh, A., Nicholas, A., Yukhananov, R., Bu, J., Wu, C.K., Geula, C., 2011. Age-related loss of calcium buffering and selective neuronal vulnerability in Alzheimer's disease. Acta neuropathologica 122, 565–576. http://dx.doi.org/10.1007/s00401-011-0865-4.

Rim, H.K., Lee, H.W., Choi, I.S., Park, J.Y., Choi, H.W., Choi, J.H., Cho, Y.W., Lee, J.Y., Lee, K.T., 2012. T-type Ca2+ channel blocker, KYS05047 induces G1 phase cell cycle arrest by decreasing intracellular Ca2+ levels in human lung adenocarcinoma A549 cells. Bioorganic & medicinal chemistry letters 22, 7123–7126. http://dx.doi.org/10.1016/j.bmcl.2012.09.076.

Sandmann, S., Spormann, J., Prenzel, F., Shaw, L., Unger, T., 2002. Calcium channel blockade limits transcriptional, translational and functional up-regulation of the cardiac calpain system after myocardial infarction. European journal of pharmacology 453, 99–109.

Sequier, J.M., Hunziker, W., Andressen, C., Celio, M.R., 1990. Calbindin D-28k Protein and mRNA Localization in the Rat Brain. The European journal of neuroscience 2, 1118–1126.

Splawski, I., Yoo, D.S., Stotz, S.C., Cherry, A., Clapham, D.E., Keating, M.T., 2006. CACNA1H mutations in autism spectrum disorders. The Journal of biological chemistry 281, 22085–22091. http://dx.doi.org/10.1074/jbc.M603316200.

Stutzmann, G.E., Smith, I., Caccamo, A., Oddo, S., Laferla, F.M., Parker, I., 2006. Enhanced ryanodine receptor recruitment contributes to Ca2+ disruptions in young, adult, and aged Alzheimer's disease mice. The Journal of neuroscience: the official journal of the Society for Neuroscience 26, 5180–5189. http://dx.doi.org/10.1523/JNEUROSCI.0739-06.2006.

Thibault, O., Landfield, P.W., 1996. Increase in single L-type calcium channels in hippocampal neurons during aging. Science 272, 1017–1020.

Toyota, M., Ho, C., Ohe-Toyota, M., Baylin, S.B., Issa, J.P., 1999. Inactivation of CACNA1G, a T-type calcium channel gene, by aberrant methylation of its 5′ CpG island in human tumors. Cancer research 59, 4535–4541.

Veeranna, Kaji, T., Boland, B., Odrljin, T., Mohan, P., Basavarajappa, B.S., Peterhoff, C., Cataldo, A., Rudnicki, A., Amin, N., Li, B.S., Pant, H.C., Hungund, B.L., Arancio, O., Nixon, R.A., 2004. Calpain mediates calcium-induced activation of the erk1,2 MAPK pathway and cytoskeletal phosphorylation in neurons: relevance to Alzheimer's disease. The American journal of pathology 165, 795–805. http://dx.doi.org/10.1016/S0002-9440(10)63342-1.

Wagner, G., Icks, A., Abholz, H.H., Schroder-Bernhardi, D., Rathmann, W., Kostev, K., 2012. Antihypertensive treatment and risk of dementia: a retrospective database study. International journal of clinical pharmacology and therapeutics 50, 195–201.